Inorg. Chem. **2005**, *44*, 9527–9533

Inorganic Chemistry

Article

Modeling the Active Site of Nitrile Hydratase: Synthetic Strategies to Ensure Simultaneous Coordination of Carboxamido-N and Thiolato-S to Fe(III) Centers

Todd C. Harrop,[†] Marilyn M. Olmstead,[‡] and Pradip K. Mascharak*,[†]

Department of Chemistry and Biochemistry, University of California, Santa Cruz, California 95064, and Department of Chemistry, University of California, Davis, California 95616

Received July 14, 2005

A general strategy for synthesizing Fe(III) complexes of ligands containing carboxamido-N and thiolato-S donors has been described. Reaction of the doubly deprotonated ligand $PyPepS^{2-}$ (where $PyPepSH_2$ = *N*-2-mercaptophenyl-2′-pyridinecarboxamide) with Fe(III) salts in DMF had previously afforded the Fe(III) complex $(Et_4N)[Fe(PyPepS)_2]$ without any problem(s) associated with autoredox reactions of the thiolate functionality. In the present work, similar reactions with the doubly deprotonated ligand $PiPepS^{2-}$ (where $PiPepSH_2$ = 2-mercapto-*N*-pyridin-2-yl-methyl-benzamide) with Fe(III) salts, however, fail to afford any Fe(III) complex because of autoredox reactions. The break in the conjugation in the $PiPepSH_2$ ligand frame is the key reason for this difference in behavior between these two very similar ligands. This is demonstrated by the fact that the same reaction with $AqPepS^{2-}$ (where $AqPepSH_2$ = 2-mercapto-*N*-quinolin-8-yl-benzamide), another ligand with extended conjugation, affords the Fe(III) complex $(Et_4N)[Fe(AqPepS)_2]$ (**1**) without any synthetic complication. It is therefore evident that ligands in which the carboxamide and thiolate functionalities are kept in conjugation could be used to isolate Fe(III) complexes with carboxamido-N and thiolato-S coordination. This finding will be very helpful in future research work in the area of modeling the active site of Fe-containing nitrile hydratase.

Introduction

The enzyme nitrile hydratase (NHase), responsible for the microbial assimilation of organic nitriles, catalyzes hydrolysis of nitriles into the corresponding amides.[1−5] The NHase active site consists of a non-heme Fe(III) or non-corrin Co(III) center with two carboxamido nitrogen and three cysteine sulfur ligands, two of which are posttranslationally modified to sulfinic ($-SO_2$) and sulfenic ($-SO$) moieties.[6−12] This unusual coordination environment of the M(III) (M = Fe, Co) center in NHase has prompted research on small molecular weight analogues in order to gain an understanding of the intrinsic properties of the active site.[13−30] However, the synthesis of such complexes under strongly basic

---

* To whom correspondence should be addressed. Email: pradip@chemistry.ucsc.edu.

[†] University of California, Santa Cruz.

[‡] University of California, Davis.

(1) Kobayashi, M.; Shimizu, S. *Curr. Opin. Chem. Biol.* **2000**, *4*, 95.
(2) Endo, I.; Odaka, M.; Yohda, M. *Trends Biotechnol.* **1999**, *17*, 244.
(3) Yamada, H.; Kobayashi, M. *Biosci., Biotechnol., Biochem.* **1996**, *9*, 1391.
(4) Kobayashi, M.; Nagasawa, T.; Yamada, H. *Trends Biotechnol.* **1992**, *10*, 402.
(5) Nagasawa, T.; Yamada, H. *Trends Biotechnol.* **1989**, *7*, 153.
(6) Nagashima, S.; Nakasako, M.; Dohmae, N.; Tsujimura, M.; Takio, K.; Masafumi, O.; Yohda, M.; Kamiya, N.; Endo, I. *Nat. Struct. Biol.* **1998**, *5*, 347.
(7) Huang, W.; Jia, J.; Cummings, J.; Nelson, M.; Schneider, G.; Lindqvist, Y. *Structure* **1997**, *5*, 691.
(8) Miyanaga, A.; Fushinobu, S.; Ito, K.; Wakagi, T. *Biochem. Biophys. Res. Commun.* **2001**, *288*, 1169.
(9) Endo, I.; Nojiri, M.; Tsujimura, M.; Nakasako, M.; Nagashima, S.; Yohda, M.; Odaka, M. *J. Inorg. Biochem.* **2001**, *83*, 247.
(10) Murakami, T.; Nojiri, M.; Nakayama, H.; Odaka, M.; Yohda, M.; Dohmae, N.; Takio, K.; Nagamune, T.; Endo, I. *Protein Sci.* **2000**, *9*, 1024.
(11) Odaka, M.; Fujii, K.; Hoshino, M.; Noguchi, T.; Tsujimura, M.; Nagashima, S.; Yohda, M.; Nagamune, T.; Inoue, Y.; Endo, I. *J. Am. Chem. Soc.* **1997**, *119*, 3785.
(12) Brennan, B. A.; Cummings, J. G.; Chase, D. B.; Turner, I. M., Jr.; Nelson, M. J. *Biochemistry* **1996**, *35*, 10068.
(13) Harrop, T. C.; Mascharak, P. K. *Acc. Chem. Res.* **2004**, *37*, 253.
(14) Kovacs, J. A. *Chem. Rev.* **2004**, *104*, 825.
(15) Mascharak, P. K. *Coord. Chem. Rev.* **2002**, *225*, 201.
(16) Tyler, L. A.; Noveron, J. C.; Olmstead, M. M.; Mascharak, P. K. *Inorg. Chem.* **2003**, *42*, 5751.
(17) Noveron, J. C.; Olmstead, M. M.; Mascharak, P. K. *J. Am. Chem. Soc.* **2001**, *123*, 3247.
(18) Tyler, L. A.; Noveron, J. C.; Olmstead, M. M.; Mascharak, P. K. *Inorg. Chem.* **2000**, *39*, 357.
(19) Noveron, J. C.; Olmstead, M. M.; Mascharak, P. K. *Inorg. Chem.* **1998**, *37*, 1138.

10.1021/ic051183z CCC: $30.25

conditions (required for the deprotonation of the carboxamide group) has not been easy, as organic thiolates have a tendency to bridge metal centers (polymerization) and undergo autoredox processes.[31−34] In most cases, the thiolate moiety serves as a reducing agent for the metal ion (Fe(III) in particular), resulting in disulfide formation and making isolation of the desired compound quite difficult. So far, two strategies have been employed to avoid this unwanted side reaction. In the first strategy, researchers employ sterically hindered thiolates to avoid the autoredox processes. For example, several Fe−NHase model compounds (some without carboxamido-N bonds) have been successfully isolated using ligands that contain *gem*-dimethyl substituents ortho to sulfur, such as (Pr,Pr)^{Me2}N$_3$(SH)$_2$,[23] H$_4$phmi,[25] and H$_5$L.[27]

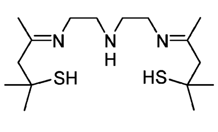
(Pr,Pr)^{Me2}N$_3$(SH)$_2$

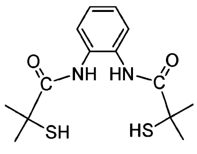
H$_4$phmi

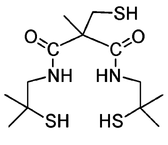
H$_5$L

The presence of *gem*-dimethyl substituents in these ligands prevents dimerization of the thiyl ($RS^{\bullet}$) radicals (generated from the transfer of one electron from the RS^- moieties to the metal center) to form disulfides.[34] We have adopted the second strategy, which employs conjugated ligand frames bearing less basic aromatic thiolates to isolate stable Fe(III) complexes.[16−19] For example, we have reported the Fe(III) complex of a tridentate ligand containing carboxamido-N and thiolato-S donors, namely (Et$_4$N)[Fe(PyPepS)$_2$] (PyPepSH$_2$ = *N*-2-mercaptophenyl-2′-pyridinecarboxamide; H's denote the dissociable carboxamide and thiol H), which forms in good yield without the occurrence of any autoredox reaction.[19]

In our continuing effort toward syntheses of model complexes of the active site of NHase, we have now designed two other tridentate ligands, namely PiPepSH$_2$ (2-mercapto-*N*-pyridin-2-yl-methylbenzamide) and AqPepSH$_2$ (2-mercapto-*N*-quinolin-8-yl-benzamide; H's represent dissociable carboxamide and thiol protons), with minor variations in the overall ligand architecture of PyPepSH$_2$.

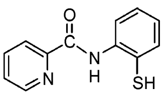
PyPepSH$_2$

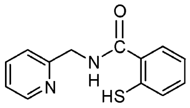
PiPepSH$_2$

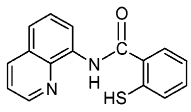
AqPepSH$_2$

In this paper, we report the synthesis, characterization, and properties of the Fe(III) and Co(III) complexes with these two new ligands. The courses of the synthetic reactions demonstrate that conjugation in these ligand frames indeed plays a critical role in the successful isolation of the desired Fe(III) complexes without any of the side reactions mentioned above. The findings of this study have implications in the ligand design and synthetic strategy of more complex ligand frames geared toward syntheses of functional models of NHase.

Experimental Section

All manipulations were carried out using standard Schlenk techniques. 8-Aminoquinoline, thiosalicylic acid, potassium ferricyanide, tetraethylammonium chloride, 2-(aminomethyl)pyridine, triethylamine, and sodium hydride were purchased from Aldrich Chemical Co. and used without further purification. (Et$_4$N)[FeCl$_4$][35] and [Co(NH$_3$)$_5$Cl]Cl$_2$ [36] were synthesized by following the published procedures. All solvents were distilled from the appropriate drying agents prior to use as follows: DMF from BaO, MeCN and CH$_2$Cl$_2$ from CaH$_2$, THF from Na/benzophenone, and Et$_2$O from Na.

PiPepSH$_2$. Step 1, PiPepS$_2$. A 30 mL mixture of 2-(aminomethyl)pyridine (1.34 g, 12.40 mmol) and triethylamine (4.58 g, 45.26 mmol) was added dropwise to a solution of 2,2′-dithiosalicyl chloride (2.14 g, 6.22 mmol) in 30 mL of CH$_2$Cl$_2$ at 4 °C. The resulting light brown solution was then allowed to stir at room temperature for 14 h. This solution was then washed with aqueous NaHCO$_3$ and NaCl. The CH$_2$Cl$_2$ layer was dried with MgSO$_4$ and filtered, and the solvent was removed by rotary evaporation to afford a brown oily residue. This oil was titrated twice with Et$_2$O (20 mL) to afford a light tan solid. Yield: 1.85 g (61%). ^{1}H NMR (CDCl$_3$, 500 MHz, δ from TMS): 8.55 (d, 1H), 7.81 (d, 1H), 7.70 (t, 1H), 7.62 (d, 1H), 7.58 (br t, 1H, NH), 7.35 (m, 2H), 7.23 (m, 2H), 4.77 (d, 2H, CH$_2$). ^{13}C NMR (CDCl$_3$, δ from TMS): 167.10 (C=O), 158.41, 148.89, 136.96, 136.74, 133.46, 131.30, 128.09, 126.04, 125.79, 122.17, 120.97, 44.72 (CH$_2$). Selected IR frequencies (KBr pellet, cm^{-1}): 3310 (ν_{NH}), 1628 (ν_{co}).

Step 2, PiPepSH$_2$. A batch of solid NaBH$_4$ (0.13 g, 3.35 mmol) was added in small portions to a degassed solution of PiPepS$_2$ (0.40 g, 0.82 mmol) in 20 mL of THF at 4 °C. The bright yellow solution was then allowed to stir at room temperature for 16 h. The solution was then concentrated to 10% of the original volume via short-path vacuum distillation, and 1 M acetic acid was added dropwise to the solution at 4 °C until the pH was 3−4. The pale yellow solid that precipitated was collected by filtration, washed with cold MeOH, and dried on a high-vacuum line for 2 h. Yield: 0.23 g (57%). ^{1}H NMR (CDCl$_3$, 500 MHz, δ from TMS): 8.76 (d, 1H),

---

(20) Shearer, J.; Jackson, H. L.; Schweitzer, D.; Rittenberg, D.; Leavy, T. M.; Kaminsky, W.; Scarrow, R. C.; Kovacs, J. A. *J. Am. Chem. Soc.* **2002**, *124*, 11417.

(21) Jackson, H. L.; Shoner, S. C.; Rittenberg, D.; Cowen, J. A.; Lovell, S.; Barnhart, D.; Kovacs, J. A. *Inorg. Chem.* **2001**, *40*, 1646.

(22) Schweitzer, D.; Ellison, J. J.; Shoner, S. C.; Lovell, S.; Kovacs, J. A. *J. Am. Chem. Soc.* **1998**, *120*, 10996.

(23) Ellison, J. J.; Nienstedt, A.; Shoner, S. C.; Barnhart, D.; Cowen, J. A.; Kovacs, J. A. *J. Am. Chem. Soc.* **1998**, *120*, 5691.

(24) Galardon, E.; Giorgi, M.; Artaud, I. *Chem. Commun.* **2004**, 286.

(25) Chatel, S.; Chauvin, A. S.; Tuchagues, J. P.; Leduc, P.; Bill, E.; Chottard, J.-C.; Mansuy, D.; Artaud, I. *Inorg. Chim. Acta* **2002**, *336*, 19.

(26) Rat, M.; Alves de Sousa, R.; Vaissermann, J.; Leduc, P.; Mansuy, D.; Artaud, I. *J. Inorg. Biochem.* **2002**, *84*, 207.

(27) Heinrich, L.; Li, Y.; Vaissermann, J.; Chottard, G.; Chottard, J.-C. *Angew. Chem., Int. Ed.* **1999**, *38*, 3526.

(28) Heinrich, L.; Mary-Verla, A.; Li, Y.; Vaissermann, J.; Chottard, J.-C. *Eur. J. Inorg. Chem.* **2001**, 2203.

(29) Heinrich, L.; Li, Y.; Provost, K.; Michalowicz, A.; Vaissermann, J.; Chottard, J.-C. *Inorg. Chim. Acta* **2001**, *318*, 117.

(30) Grapperhaus, C. A.; Li, M.; Patra, A. K.; Poturovic, S.; Kozlowski, P. M.; Zgierski, M. Z.; Mashuta, M. S. *Inorg. Chem.* **2003**, *42*, 4382.

(31) Millar, M.; Lee, J. F.; Fikar, R. *Inorg. Chim. Acta* **1996**, *243*, 333.

(32) Dance, I. G. *Polyhedron* **1986**, *5*, 1037.

(33) Herskovitz, T.; Depamphilis, B. V.; Gillum, W. O.; Holm, R. H. *Inorg. Chem.* **1975**, *14*, 1426.

(34) Ellis, K. J.; Lappin, A. G.; McAuley, A. *J. Chem. Soc., Dalton Trans.* **1975**, 1930.

(35) Gill, N. S.; Taylor, F. B. *Inorg. Synth.* **1967**, *9*, 136.

(36) Schlessinger, G. C. *Inorg. Synth.* **1967**, *9*, 160.

7.95 (t, 1H), 7.80 (d, 1H), 7.52 (d, 1H), 7.43 (t, 1H), 7.30 (m, 3H, ArH and NH), 7.16 (t, 1H), 5.04 (d, 2H, CH_2), 4.62 (s, 1H, SH). ^{13}C NMR ($CDCl_3$, δ from TMS): 168.63 (C=O), 155.40, 149.59, 140.56, 133.10, 132.04, 131.39, 131.19, 128.11, 127.02, 125.41, 124.27, 42.72 (CH_2). Selected IR frequencies (KBr pellet, cm^{-1}): 3314 (ν_{NH}), 2544 (ν_{SH}), 1638 (ν_{co}).

$AqPepSH_2$. Step 1, $AqPepS_2$. A solution of 1.68 g (11.68 mmol) of 8-aminoquinoline and 5.20 g (51.40 mmol) of triethylamine in 30 mL of CH_2Cl_2 was added dropwise to a solution of 2.01 g (5.85 mmol) of 2,2′-dithiosalicyl chloride in 30 mL of CH_2Cl_2 at 4 °C. The resulting light brown solution was then heated to reflux for 4 h. After being stirred at room temperature overnight, the brown solution was washed with aqueous $NaHCO_3$ and NaCl. The CH_2Cl_2 layer was then dried with $MgSO_4$ and filtered, and the solvent was removed by rotary evaporation to afford a brown oil. This oil was allowed to stir in 50 mL of a MeOH/Et_2O (1:1) solution for 12 h, a step that eventually resulted in the precipitation of a pale yellow solid. Yield: 1.86 g (57%). ^1H NMR ($CDCl_3$, 500 MHz, δ from TMS): 10.62 (s, 1H, NH), 8.97 (d, 1H), 8.83 (d, 1H), 8.20 (d, 1H), 7.97 (d, 1H), 7.87 (d, 1H), 7.60 (m, 2H), 7.48 (t, 1H), 7.44 (t, 1H), 7.34 (t, 1H). ^{13}C NMR ($CDCl_3$, δ from TMS): 165.99 (C=O), 148.43, 138.77, 138.64, 136.61, 134.44, 133.96, 131.85, 128.13, 127.71, 127.60, 127.48, 126.22, 122.19, 121.84, 117.04. Selected IR frequencies (KBr pellet, cm^{-1}): 3339 (ν_{NH}), 1660 (ν_{co}).

Step 2, $AqPepSH_2$. A solution of 1.00 g (1.80 mmol) of $AqPepS_2$ in 20 mL of degassed THF was cooled to 4 °C. A batch of solid $NaBH_4$ (0.28 g, 7.26 mmol) was added to this solution in small portions. The bright red solution thus obtained was stirred for 4 h at room temperature. The solution was then concentrated via short-path vacuum distillation to 10% of its original volume, and 1 M acetic acid was slowly added to this solution at 4 °C until the pH was 3−4. The light yellow solid that almost immediately precipitated was collected by filtration on a frit, washed with cold Et_2O, and dried under high vacuum for 2 h. Yield: 0.20 g (80%). ^1H NMR ($CDCl_3$, 500 MHz, δ from TMS): 10.56 (s, 1H, NH), 8.95 (d, 1H), 8.85 (d, 1H), 8.26 (d, 1H), 7.86 (d, 1H), 7.63 (m, 2H), 7.52 (m, 1H), 7.43 (d, 1H), 7.37 (t, 1H), 7.31 (t, 1H), 4.73 (s, 1H, SH). ^{13}C NMR ($CDCl_3$, δ from TMS): 166.84 (C=O), 148.07, 137.17, 134.57, 131.53, 131.13, 128.39, 128.25, 127.76, 125.47, 122.25, 121.74, 117.72. Selected IR frequencies (KBr pellet, cm^{-1}): 3339 (ν_{NH}), 2521 (ν_{SH}), 1651 (ν_{co}).

$(Et_4N)[Fe(AqPepS)_2]$ (1). To a degassed solution of 0.13 g (0.47 mmol) of $AqPepSH_2$ in 15 mL of DMF was added a batch of NaH (0.03 g, 1.21 mmol), and the solution was allowed to stir until all the NaH had reacted. The solution was then cooled to −40 °C. Next, a solution of 0.08 g (0.23 mmol) of $(Et_4N)[FeCl_4]$ in 2 mL of DMF was slowly added to the cold solution containing the deprotonated ligand. The resulting dark red mixture was then allowed to slowly warm to room temperature overnight. After 12 h, the reaction mixture was concentrated to ∼50% of the original volume, and was filtered to remove NaCl. Next, a 5 mL portion of degassed Et_2O was added to this solution, and the mixture was placed in the freezer for 12 h. The resulting red microcrystalline solid was collected and dried under high vacuum for 2 h. Yield: 0.10 g (59%). Selected IR frequencies (KBr pellet, cm^{-1}): 1568 (vs, ν_{co}). Absorption spectrum in MeCN: λ_{max} (ϵ, M^{-1} cm^{-1}) 720 (sh 1220), 623 (3820), 490 (5300), 355 (sh 10 000).

$(Et_4N)[Co(PiPepS)_2]$ (2). A batch of 0.048 g (2.00 mmol) of NaH was added to a solution of 0.20 g (0.82 mmol) of $PiPepSH_2$ in 15 mL of degassed DMF, and the mixture was stirred until all the NaH had reacted (∼20 min). To the bright yellow solution was then added a batch of 0.10 g (0.41 mmol) of $[Co(NH_3)_5Cl]Cl_2$, and the mixture was heated to 65 °C for 4 h. During this time, the mixture slowly became homogeneous and developed a dark red-brown color. Next, a batch of Et_4NCl (0.10 g, 0.62 mmol) was added, and the solution was further stirred at room temperature for 10 h. The solvent was then removed in vacuo, and the dark red residue was dissolved in 30 mL of MeCN. It was filtered to remove NaCl; 10 mL of Et_2O was then added to the filtrate, and the mixture was stored at −20 °C for 18 h. The resulting microcrystalline product was collected by filtration, washed with cold Et_2O, and dried under vacuum. Yield: 0.16 g (59%). ^1H NMR (DMSO-d_6, 500 MHz, δ from TMS): 7.95 (d, 1H), 7.79 (d, 1H), 7.59 (t, 1H), 7.51 (d, 1H), 6.99 (t, 1H), 6.89 (d, 1H), 6.64 (m, 2H), 5.24 (q, 2H, CH_2), 3.19 (q, 4H, CH_2 of Et_4N), 1.15 (t, 6H, CH_3 of Et_4N). Selected IR frequencies (KBr pellet, cm^{-1}): 1516 (vs, ν_{co}). Absorption spectrum in MeCN: λ_{max} (ϵ, M^{-1} cm^{-1}) 600 (sh, 1040), 495 (2250).

$(Et_4N)[Co(AqPepS)_2]$ (3). A batch of NaH (0.08 g, 3.15 mmol) was added to a solution of $AqPepSH_2$ (0.31 g, 1.09 mmol) and dissolved in 15 mL of DMF; the solution was stirred until all the NaH had reacted (∼20 min). To the resultant bright orange solution was added 0.14 g (0.55 mmol) of $[Co(NH_3)_5Cl]Cl_2$ followed by Et_4NCl (0.11 g, 0.68 mmol), and the mixture was warmed at 65 °C for 4 h. The deep red solution thus obtained was allowed to stir at room temperature overnight. Next, the DMF solution was removed by short-path vacuum distillation to afford a dark red oily material. This oil was redissolved in 50 mL of MeCN, and filtered to remove NaCl. The filtrate was then concentrated to 15 mL, and placed at −20 °C for 12 h. The dark red crystalline material thus obtained was collected on a frit, and dried under high vacuum for 2 h. Yield: 0.26 g (63%). Selected IR frequencies (KBr pellet, cm^{-1}): 1574 (vs, ν_{co}). Absorption spectrum in MeCN: λ_{max} (ϵ, M^{-1} cm^{-1}) 670 (sh, 470), 525 (sh, 950), 410 (2700).

Physical Measurements. Electronic absorption spectra were recorded on a Perkin-Elmer Lambda 9 spectrophotometer. Infrared spectra were obtained with a Perkin-Elmer 1600 or Spectrum 1 FTIR spectrophotometer. EPR spectra were recorded at X-band frequencies with a Bruker EleXsys E500 spectrometer at liquid N_2 temperature. ^1H NMR spectra were recorded at 298 K on a Varian Unity Plus 500 spectrometer running Solaris 2.6/VNMR 6.1B. Electrochemical measurements were performed with Princeton Applied Research instrumentation (model 273A) at 298 K in DMF using 0.1 M $(Et_4N)(ClO_4)$ as the supporting electrolyte. The working electrode was a Beckman Pt-inlay working electrode, and the potentials were measured versus a saturated calomel electrode (SCE).

X-ray Data Collection and Structure Solution and Refinement. Black plates of $(Et_4N)[Fe(AqPepS)_2]$ (**1**) were obtained by slow diffusion of Et_2O into a DMF solution of the complex under anaerobic conditions. Red needles of $(Et_4N)[Co(PiPepS)_2]\cdot CH_3CN$ (**2**$\cdot CH_3CN$) were grown via slow cooling of a saturated MeCN/Et_2O (1:1) solution of the complex to −20 °C. Black blocks of $(Et_4N)[Co(AqPepS)_2]\cdot 0.5CH_3CN\cdot 0.5H_2O$ (**3**$\cdot 0.5CH_3CN\cdot 0.5H_2O$) were grown from slow evaporation of a MeCN solution of the complex at room temperature. Diffraction data for the complexes were collected at 90 K on a Bruker SMART 100 system. Mo Kα (0.71073 Å) radiation was used, and the data were corrected for absorption effects. The structures were solved by direct methods (SHELXS-97). Machine parameters, crystal data, and data collection parameters for **1**−**3** are summarized in Table 1, whereas selected bond distances and angles are listed in Table 2. Complete crystallographic data for $(Et_4N)[Fe(AqPepS)_2]$ (**1**), $(Et_4N)[Co(PiPepS)_2]\cdot CH_3CN$ (**2**$\cdot CH_3CN$), and $(Et_4N)[Co(AqPepS)_2]\cdot 0.5CH_3CN\cdot 0.5\ H_2O$ (**3**$\cdot 0.5CH_3CN\cdot 0.5H_2O$) are included in the Supporting Information.

Table 1. Summary of Crystal Data and Intensity Collection and Structural Refinement Parameters for $(Et_4N)[Fe(AqPepS)_2]$ (**1**), $(Et_4N)[Co(PiPepS)_2]\cdot CH_3CN$ (**2**$\cdot CH_3CN$), and $(Et_4N)[Co(AqPepS)_2]\cdot 0.5CH_3CN\cdot 0.5\ H_2O$ (**3**$\cdot 0.5CH_3CN\cdot 0.5H_2O$)

	1	**2**	**3**
formula	$C_{40}H_{40}N_5O_2S_2Fe$	$C_{36}H_{43}N_6O_2S_2Co$	$C_{41}H_{42.50}N_{5.50}O_{2.50}S_2Co$
mol wt	742.74	714.81	775.35
cryst color, habit	black plate	red needle	black block
T (K)	93(2)	91(2)	93(2)
cryst syst	monoclinic	triclinic	monoclinic
space group	$C2/c$	$P\bar{1}$	$C2/c$
a (Å)	21.9615(14)	10.2093(5)	23.046(4)
b (Å)	10.4517(7)	13.1439(6)	12.307(2)
c (Å)	15.9058(11)	13.3073(6)	25.936(4)
α (deg)	90	108.6560(10)	90
β (deg)	108.985(2)	94.8890(10)	90.967(4)
γ (deg)	90	94.9520(10)	90
V (Å^3)	3452.3(4)	1673.48(14)	7355(2)
Z	4	2	8
d_{calcd} (g cm^{-3})	1.429	1.419	1.400
abs coeff (μ, mm^{-1})	0.603	0.681	0.627
GOF[a] on F^2	1.069	1.012	1.039
R_1[b] (%)	3.22	4.36	4.16
R_{w2}[c] (%)	8.58	9.23	9.71

[a] GOF $= \{[\sum w(F_o^2 - F_c^2)^2]/(M - N)\}^{1/2}$ (M = no. of reflections, N = no. of parameters refined). [b] $R_1 = \sum||F_o| - |F_c||/\sum|F_o|$. [c] $R_{w2} = \{[\sum w(F_o^2 - F_c^2)^2]/[\sum w(F_o)^2]\}^{1/2}$.

Table 2. Selected Bond Distances (Å) and Angles (deg)

	Complex **1**		
Fe(1)−N(1)	1.9902(10)	N(1)−C(8)	1.4087(14)
Fe(1)−N(2)	2.0001(10)	N(2)−C(16)	1.3696(14)
Fe(1)−S(1)	2.2189(3)	C(6)−C(7)	1.5043(16)
S(1)−C(1)	1.7533(12)	C(1)−C(2)	1.4071(17)
O(1)−C(7)	1.2451(15)	C(8)−C(9)	1.3966(15)
N(1)A−Fe(1)−N(1)	171.64(6)	N(1)A−Fe(1)−S(1)	91.86(3)
N(1)A−Fe(1)−N(2)	92.06(4)	N(1)−Fe(1)−S(1)	93.82(3)
N(1)−Fe(1)−N(2)	81.84(4)	N(2)−Fe(1)−S(1)	174.18(3)
N(2)−Fe(1)−N(2)A	86.53(6)	N(2)A−Fe(1)−S(1)	89.77(3)
S(1)−Fe(1)−S(1)A	94.268(18)	C(1)−S(1)−Fe(1)	104.31(4)
	Complex **2**		
Co−N(1)	1.9376(16)	Co−S(2)	2.2134(5)
Co−N(2)	1.9786(17)	O(1)−C(7)	1.262(2)
Co−N(3)	1.9408(17)	S(1)−C(1)	1.746(2)
Co−N(4)	1.9849(16)	N(1)−C(8)	1.469(3)
Co−S(1)	2.2100(5)	N(3)−C(21)	1.466(3)
N(1)−Co−N(3)	176.48(7)	N(1)−Co−S(1)	95.61(5)
N(1)−Co−N(2)	84.04(7)	N(2)−Co−S(1)	178.33(5)
N(3)−Co−N(2)	93.88(7)	S(1)−Co−S(2)	89.39(2)
N(1)−Co−N(4)	93.73(7)	C(1)−S(1)−Co	110.35(7)
N(3)−Co−N(4)	83.45(7)	N(3)−C(21)−C(22)	110.06(17)
	Complex **3**		
Co−N(1)	1.9432(14)	Co−S(2)	2.2012(6)
Co−N(2)	1.9703(15)	O(1)−C(7)	1.244(2)
Co−N(3)	1.9459(15)	S(1)−C(1)	1.7394(19)
Co−N(4)	1.9731(16)	N(1)−C(8)	1.407(2)
Co−S(1)	2.1905(6)	C(8)−C(9)	1.393(2)
N(1)−Co−N(3)	173.29(7)	N(2)−Co−N(4)	86.99(6)
N(1)−Co−N(2)	84.37(6)	N(1)−Co−S(1)	96.73(5)
N(3)−Co−N(2)	91.01(6)	N(2)−Co−S(1)	177.35(5)
N(1)−Co−N(4)	90.67(6)	S(1)−Co−S(2)	92.43(2)
N(3)−Co−N(4)	84.22(7)	C(1)−S(1)−Co	109.56(7)

Results and Discussion

In previous accounts, we have demonstrated that Fe(III) complexes of ligands containing carboxamide and thiolate groups (e.g., $PyPepSH_2$) can be synthesized via the reaction of the deprotonated ligand (with NaH) with Fe(III) salts such as $(Et_4N)[FeCl_4]$ in solvents such as DMF.[17,19] However, under anaerobic and anhydrous conditions, reaction of $(Et_4N)[FeCl_4]$ with $PiPepS^{2-}$ (deprotonated with NaH) in DMF invariably resulted in autoredox processes leading to the formation of disulfide (see the Supporting Information) and Fe(II) species (Scheme 1).[32−34] When the reaction was performed at −40 °C, an initial short-lived red-violet color (most likely due to the Fe(III) complex $(Et_4N)[Fe(PiPepS)_2]$) was observed. The color, however, bleached within minutes. Substitution of the Fe(III) starting salt to $[Fe(DMF)_6](ClO_4)_3$ also resulted in similar transient red-colored species followed by bleaching. To eliminate such autoredox reaction, we attempted an alternate route to this Fe(III) complex, namely reaction of a DMF solution of $PiPepS^{2-}$ with Fe(II) salts such as $[Fe(MeCN)_4](ClO_4)_2$, followed by in situ oxidation with ferrocenium tetrafluoroborate ($FcBF_4$). This method also did not work, and only intractable pale brown materials were left in the reaction flasks at the end of the reaction. So far, all attempts to isolate $(Et_4N)[Fe(PiPepS)_2]$ have failed in our hands. We believe that incorporation of the CH_2 group between the pyridine ring and carbonyl carbon results in enhancement of the unwanted autoredox reaction. Loss of conjugation in the ligand frame hinders stabilization of the negative charges of $PiPepS^{2-}$ (unlike $PyPepS^{2-}$), and allows electron transfer to the metal ion. The break in conjugation also makes the thiolato-S moiety of $PiPepS^{2-}$ considerably more nucleophilic (hence a better reducing agent) compared to a more-conjugated thiolato-S moiety of $PyPepS^{2-}$.

The CH_2 group between the pyridine ring and carbonyl carbon of $PiPepS^{2-}$ could also lead to secondary redox activity. Results from this laboratory have shown that such CH_2 groups themselves are susceptible toward oxidation when coordinated to Co(III) or Fe(III) centers in similar ligand frames without thiolato-S donors.[37] For instance, reaction of Fe(III) salts with the deprotonated carboxamide ligand pmpH in air resulted in the formation of $[Fe(bpca)_2]^+$ with the methylene CH_2 unit being converted into a carbonyl C═O group.[37] The reactivity of the CH_2 group in the Fe(III) complex of pmp^- arises from the tendency to achieve conjugation throughout the ligand frame via conversion to $bpca^-$. In the absence of air, this reaction does not proceed, and only brown intractable materials are isolated. Although the presence of a thiolate group in $PiPepS^{2-}$ prevented us from checking this possibility,[38] one expects similar complications from the CH_2 group between the pyridine ring and carbonyl carbon in the ligand frame.

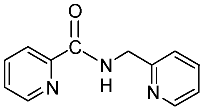
pmpH

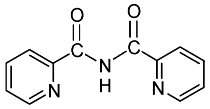
bpcaH

---

(37) Rowland, J. M.; Olmstead, M. M.; Mascharak, P. K. *Inorg. Chem.* **2002**, *41*, 2754.

(38) Both O_2 and H_2O_2 react first with the thiolato-S centers of the iron complexes and lead to complicated side reactions. In case of the cobalt complexes, the thiolato-S centers are oxidized to the corresponding sulfinic groups (as reported in refs 16 and 18). We were therefore unable to determine whether oxidation of the CH_2 unit occurred.

Scheme 1. Reactivity of Fe(III) Salts with the Ligands $AqPepSH_2$ (top) and $PiPepSH_2$ (bottom)

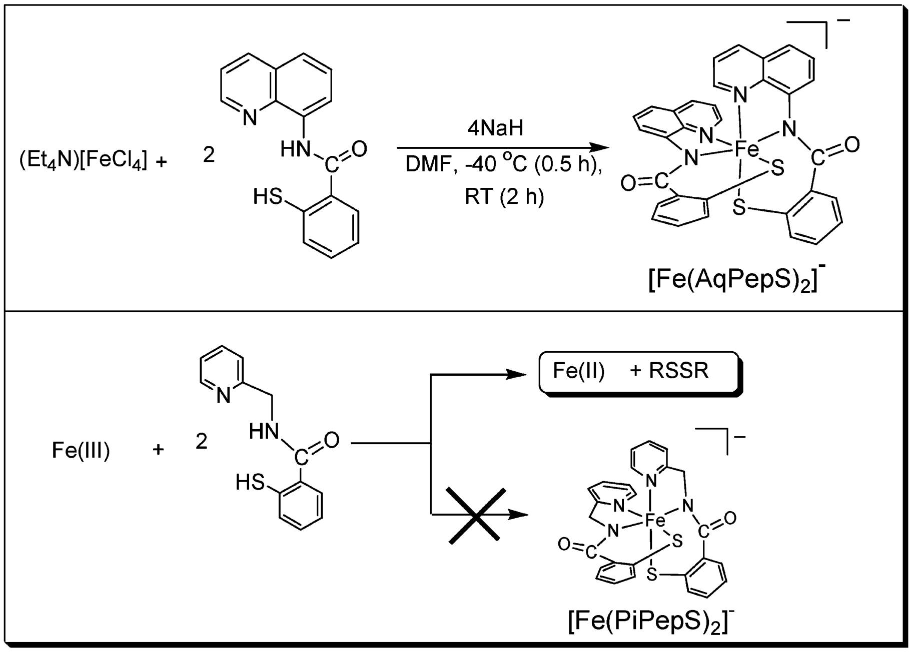

If our hypothesis is correct, then incorporation of the CH_2 group into a conjugated frame should result in an isolable Fe(III) complex. To test this possibility, we have also synthesized an analogous ligand frame, namely $AqPepSH_2$, that contains the exact same donor set (and chelate ring size) with the exception of a conjugated benzene ring in place of the methylene CH_2 group of $PiPepSH_2$. Indeed, in contrast to the Fe(III) chemistry with $PiPepSH_2$, the reaction of $AqPepSH_2$ with Fe(III) salts followed the normal route that we have previously observed with $PyPepSH_2$ (Scheme 1). Reaction of $(Et_4N)[FeCl_4]$ with a cold (−40 °C) DMF solution of $AqPepS^{2-}$ (deprotonated with NaH) cleanly afforded the deep red Fe(III) complex $(Et_4N)[Fe(AqPepS)_2]$ (**1**) in good yield. No other side products resulting from autoredox processes were observed in the course of the reaction. It is therefore evident that conjugation in ligand frame is essential in ligands of this type in order to isolate their iron complexes.

Our conclusion is further supported by the reactions of the two ligands $PiPepSH_2$ and $AqPepSH_2$ with Co(III) salts. Because the Co(III) center resists reduction to a great extent, reactions of the deprotonated ligands with Co(III) salts such as $[Co(NH_3)_5Cl]Cl_2$ are not beset with problems caused by autoredox reactions. Reaction of $[Co(NH_3)_5Cl]Cl_2$ with a warm (65 °C) solution of 2 equiv of the deprotonated (via NaH) $PiPepS^{2-}$ ligand in DMF resulted in a deep red-brown solution over a period of ~4 h. Addition of Et_4NCl and further workup afforded dark red crystalline $(Et_4N)[Co(PiPepS)_2]$ (**2**) in good yield. The second Co(III) complex, $(Et_4N)[Co(AqPepS)_2]$ (**3**), has also been isolated via a similar reaction. We like to point out here that this observation is quite in line with the synthesis of the Co(III) complex with the ligand pmp^-, which is readily isolated even in the presence of air.[37] Only the use of strong oxidants such as H_2O_2 converts the Co(III) complex $[Co(pmp)_2]^+$ into $[Co(bpca)_2]^+$. It thus appears that the CH_2 group of $PiPepS^{2-}$ is also less sensitive to oxidation when coordinated to a Co(III) center.

Structure and Properties. Crystallographic analysis of **1** reveals that the Fe(III) center resides in a N_4S_2 ligand environment with distorted octahedral geometry formed by the two $AqPepS^{2-}$ ligands (Figure 1). The two $AqPepS^{2-}$ ligands bind to the Fe(III) center in mer fashion with the two carboxamido-N moieties occupying trans positions. The two thiolato-S donors are cis to each other. In **1**, the average $Fe-N_{amido}$ bond length (1.9902(10) Å) lies within the expected range observed for other $Fe-N_{amido}$ bonds.[16−29,39] Interestingly, the average Fe−S bond distance (2.2189(3) Å) is slightly shorter than the Fe−S bond lengths found in the similar complex $(Et_4N)[Fe(PyPepS)_2]$ (avg: 2.229(11) Å)[19] despite a bigger ring size (6 vs 5). These bond distances are all within the range observed for Fe−NHase.[6,7]

The low-spin Fe(III) center of Fe−NHase exhibits a green color arising from an ~700 nm S-to-Fe(III) charge-transfer band in its electronic absorption spectrum.[12] The electronic absorption spectrum of **1** in MeCN displays a series of overlapping peaks in the visible region. The low-energy band at 720 nm ($\epsilon = 1220\ M^{-1}\ cm^{-1}$) is consistent with other six-coordinate Fe(III) species containing thiolato-S coordination, and has been assigned as thiolate-to-Fe(III) charge transfer (LMCT).[17,19,23,27,40] In addition, the overlapping bands in the 490−625 nm region also arise from various charge-transfer transitions. The X-band EPR spectrum of **1** in DMF glass clearly indicates that the Fe(III) center in this complex is low-spin and exists in an asymmetric coordination environment ($g = 2.23$, 2.16, and 1.98, Figure 2). Magnetic susceptibility measurements on **1** also confirm the presence of the low-spin nature of the Fe(III) center at room temperature ($\mu_B = 1.98\ \mu_B$, polycrystalline sample). Elec-

---

(39) Marlin, D. S.; Mascharak, P. K. *Chem. Soc. Rev.* **2000**, *29*, 69.

(40) Kennepohl, P.; Neese, F.; Schweitzer, D.; Jackson, H. L.; Kovacs, J. A.; Solomon, E. I. *Inorg. Chem.* **2005**, *44*, 1826.

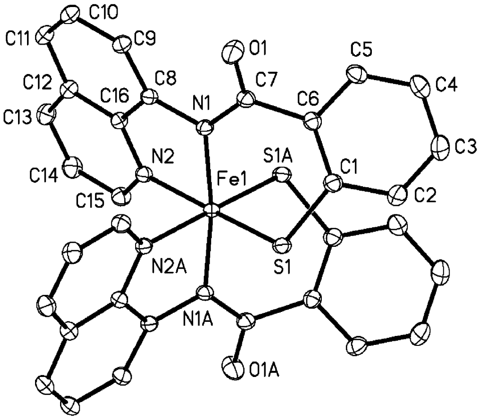

Figure 1. Thermal ellipsoid plot (50% probability) of the anion of **1**. H atoms omitted for the sake of clarity.

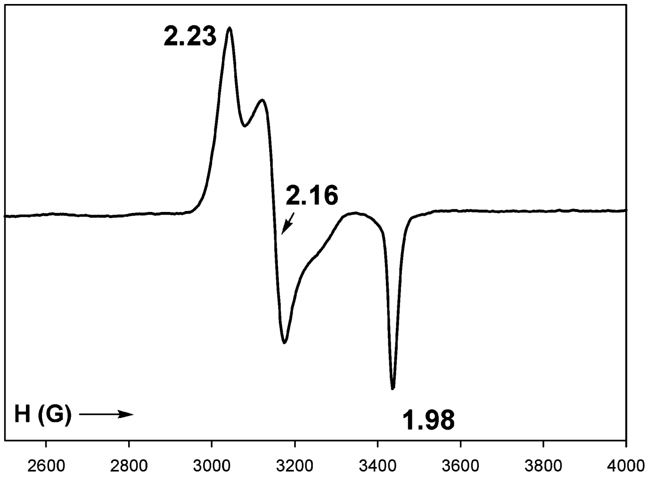

Figure 2. X-Band EPR spectrum of **1** in DMF glass at 120 K. Selected *g* values are indicated. Spectrometer settings: microwave frequency, 9.50 GHz; microwave power, 20 mW; modulation frequency, 100 kHz; modulation amplitude, 5 G.

trochemical studies reveal a highly negative half-wave potential ($E_{1/2}$) for the Fe(III)/Fe(II) couple of **1** at −1.06 V vs SCE (DMF). This value is close to the $E_{1/2}$ value of $(Et_4N)[Fe(PyPepS)_2]$ (−1.12 V vs SCE, DMF). Ligation of carboxamido-N and thiolato-S donors provides a high degree of stability to the Fe(III) centers in these types of complexes.[17,19,39]

The structure of the anion of **2** is shown in Figure 3. The two deprotonated $PiPepS^{2-}$ ligands are coordinated to the Co(III) center in mer fashion, and the geometry around cobalt is distorted octahedral. Unlike $(Me_4N)[Co(PyPepS)_2]$, in which the $PyPepS^{2-}$ ligands are essentially planar because of extensive delocalization,[18] $(Et_4N)[Co(PiPepS)_2]$ displays a slight tilt of the benzene thiolate rings (Figure 3). We presume that this tilting arises from the loss of conjugation in the $PiPepS^{2-}$ ligand frame due to the incorporation of the CH_2 moiety. Also, the C1−S1−Co angle (110.35(7)°) of $[Co(PiPepS)_2]^-$ is greater than the same angle in $[Co(PyPepS)_2]^-$ (C12−S1−Co: 97.06(13)°).[18] This widening is attributed to the presence of six-membered chelate rings in **2** ($[Co(PyPepS)_2]^-$ contains five-membered rings). Structurally, **2** is very similar to the other Co(III) complexes reported by us with similar donor sets,[16,18] and exhibits average Co−N_{amido} and Co−S bond distances of 1.9392(16) and 2.2119(5) Å, respectively.

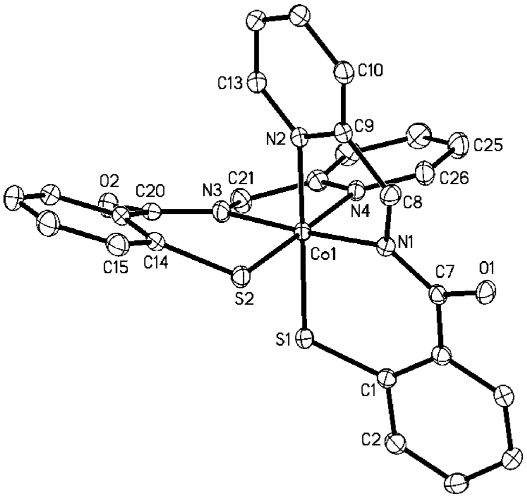

Figure 3. Thermal ellipsoid plot (50% probability) of the anion of **2**. H atoms omitted for the sake of clarity.

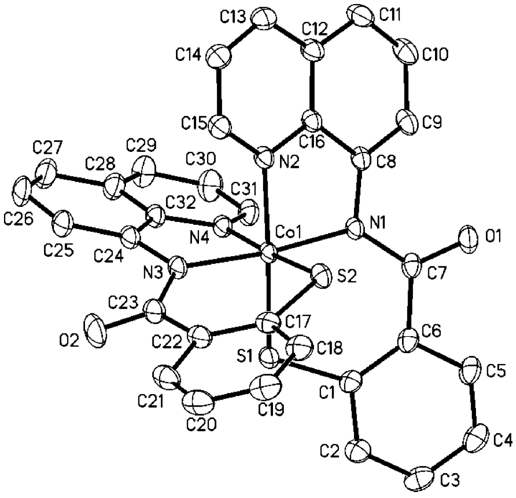

Figure 4. Thermal ellipsoid plot (50% probability) of the anion of **3**. H atoms omitted for the sake of clarity.

The Co(III) center of **3** also resides in a distorted octahedral geometry with two $AqPepS^{2-}$ ligands coordinated in mer fashion (Figure 4). Overall, the metric parameters of **3** are very similar to those of its nonconjugated analogue **2**. For example, the average Co−N_{amido} and Co−S bond distances are 1.9456(14) and 2.1959(6) Å, respectively, and the C1−S1−Co angle is 109.56(7)°. One interesting aspect of the structure is the tilt of the benzene thiolato rings (Figure 4) despite the highly conjugated $AqPepS^{2-}$ ligand frame.

The deep red color ($\lambda_{max} \sim 500$ nm) of the solutions of **2** and **3** in MeCN arises from thiolate-to-Co(III) (LMCT) charge-transfer transitions. Similar LMCT bands have been observed in other Co(III) complexes with carboxamido-N and thiolato-S coordination.[18,26,28,29] The low-spin Co(III) centers in **2** and **3** with $S = 0$ ground state exhibit clean ^1H NMR spectra of the complexes in DMSO-d_6 (Figure S1). Additionally, the Co(III) centers of **2** and **3** are difficult to reduce electrochemically, and display no reduction wave down to −1.8 V vs SCE in DMF.

Conclusion

It is now quite clear that the synthesis and isolation of Fe(III) complexes is not quite straightforward when it comes to complexation with ligands containing carboxamido-N and thiolato-S donors. The relatively small amount of complexes that do exist attests to this conclusion.[17,19,24,27] The fact that we were able to isolate and structurally characterize the Fe(III) complex with the ligand $AqPepSH_2$ (and $PyPepSH_2$[19]) but not $PiPepSH_2$ provides clues in regard to the design and syntheses of future ligands for modeling the active site of the Fe−NHases. It is evident that successful isolation of Fe(III) complexes with bound carboxamido-N and thiolato-S donors without any potential autoredox side reactions is possible when these groups are part of a conjugated ligand frame. The other option is to include *gem*-dimethyl substituents ortho to the thiolato-S donor center.[24,27] Once formed, these low-spin Fe(III) complexes are highly stable in the +3 oxidation state, and exhibit electronic absorption spectra that resemble the absorption spectrum of Fe−NHase. Syntheses of the corresponding Co(III) complexes are, however, much less susceptible to the side reactions, and hence the ligand requirements are less stringent.

Acknowledgment. T.C.H. received support from NIH IMSD Grant GM58903.

Supporting Information Available: ^1H NMR (500 MHz) spectrum of **2** in DMSO-d_6 (Figure S1), FTIR (KBr matrix) and ^1H NMR spectrum (in $CDCl_3$) of the disulfide $(PiPepS)_2$ isolated from the reaction mixture of Fe(III) and $PiPepSH_2$ (Figures S2 and S3), and X-ray crystallographic data (in CIF format) and tables for the structure determination of complexes $(Et_4N)[Fe(AqPepS)_2]$ (**1**), $(Et_4N)[Co(PiPepS)_2]\cdot CH_3CN$ (**2**$\cdot CH_3CN$), and $(Et_4N)[Co(AqPepS)_2]\cdot 0.5CH_3CN\cdot 0.5H_2O$ (**3**$\cdot 0.5CH_3CN\cdot 0.5H_2O$). This material is available free of charge via the Internet at http://pubs.acs.org.

IC051183Z